

Figure 1. Comparison of normal and pathological alternative splicing in healthy and degenerating neurons, showing how disrupted splice regulation can produce pathogenic protein isoforms or trigger nonsense-mediated decay.

The U1 small nuclear RNA (snRNA) is a key component of the spliceosome, responsible for recognizing the 5' splice site and initiating spliceosome assembly³. Within U1, the Stem-Loop IV (SLIV) domain plays a critical role in: bridging interactions between spliceosomal components, regulating exon recognition, and influencing splicing efficiency and fidelity.

Background

Alternative splicing allows a single gene to produce multiple protein isoforms through selective exon inclusion or exclusion. In neurons, precise splicing regulation is critical, and splicing defects are linked to neurodegenerative diseases including Alzheimer's disease, ALS, and frontotemporal dementia¹.

The MAPT gene encodes the tau protein, where alternative splicing of exon 10 produces 3R tau (exon exclusion) or 4R tau (exon inclusion)². Disruption of this balance contributes to tau pathology and neurodegeneration. Exon 10 recognition depends partly on U1 snRNA interactions at the 5' splice site.

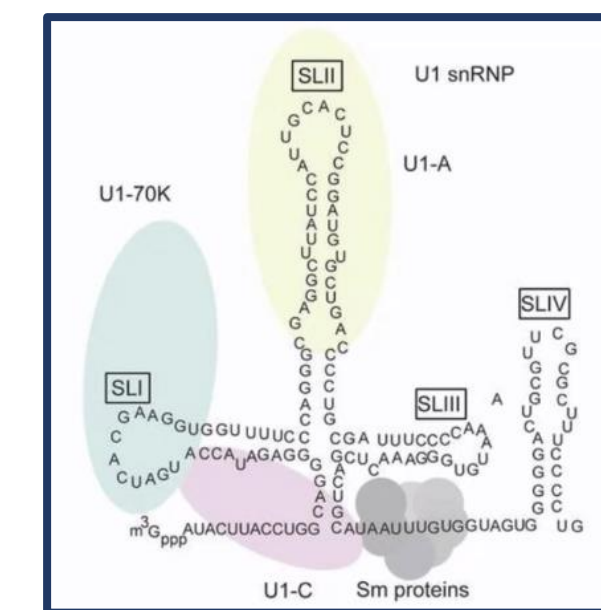


Figure 2. Structure of the U1 snRNP complex

Our Solution

In this project, engineered U1 snRNAs were designed to stabilize splice-site recognition and promote controlled MAPT exon 10 inclusion as a potential RNA-based therapeutic strategy.

Design Visual from ViennaRNA								
Design 1	Design 2	Design 3	Design 4	Design 5	Design 6	Design 7	Design 8	Design 9
Wild Type MFE: -55	No Inner Loop MFE: -62.4	No Inner Loop + Closing BP + Tail MFE: -64.5	Multi MFE: -60.099998	GC Stem MFE: -68.0	CG Stem MFE: -68.5	GCC Stem MFE: -67.3	CCG Stem MFE: -66.1	Short Stem MFE: -47.9

Figure 3. Our 8 engineered U1 snRNA variants and the wildtype, with the two successful designs highlighted in blue. Changes in Design 3 include changing the inner loop, changing the closing base pairs of the tetraloop to CG, and changing U to A on the tail. Design 4 keeps the inner loop, changes all closing base pairs to CG, changes the tetraloop to a more stable version from literature, and changes U to A on the tail. ViennaRNA was used to visualize the designs and predicted the minimum free energy (MFE), which needed to be less than the wildtype's -55.

Our Workflow

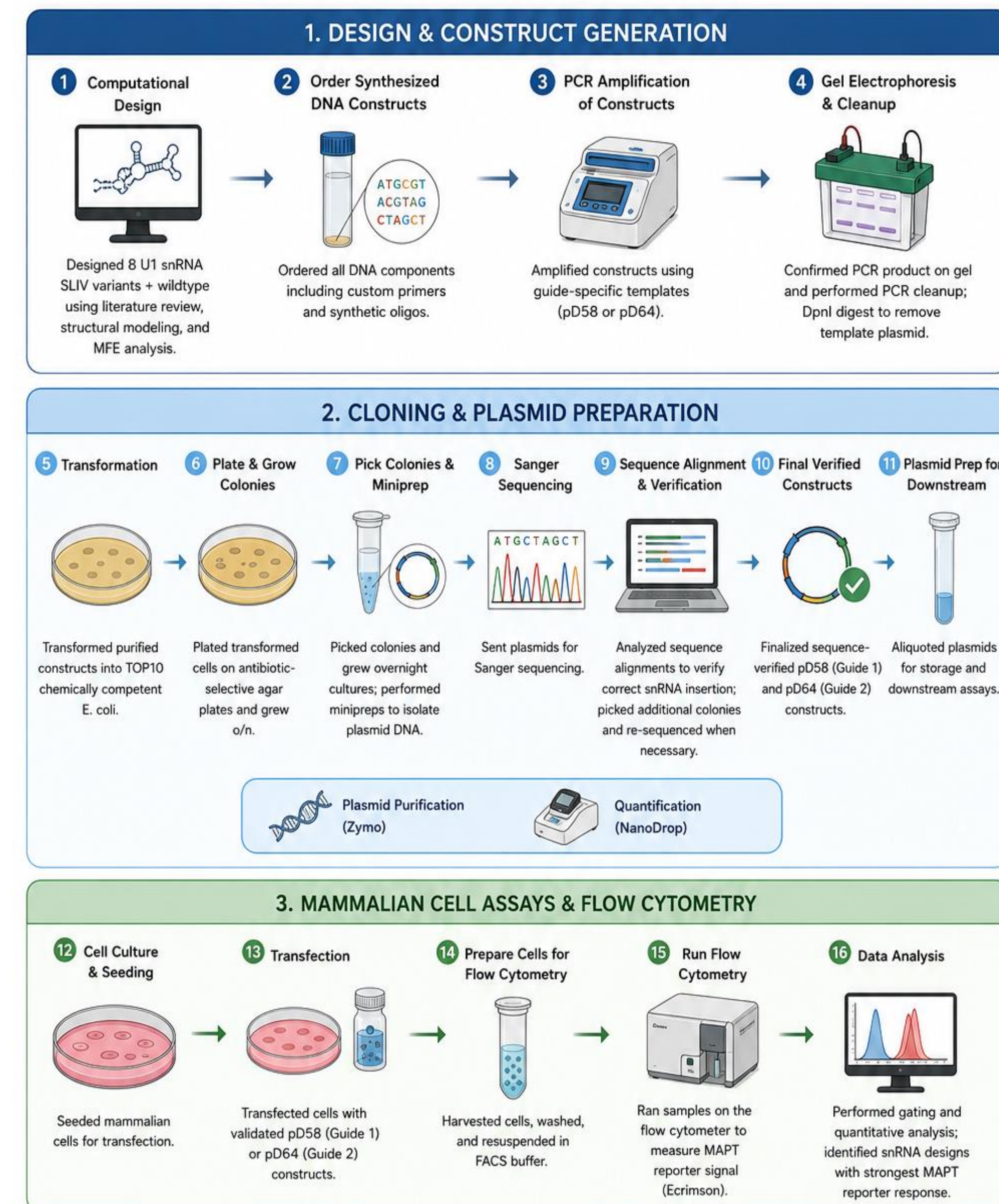


Figure 4. Details of our workflow that included 3 main stages: design and construct generation, cloning and plasmid preparation, and mammalian cell assays and flow cytometry, followed by data analysis

Data Analysis

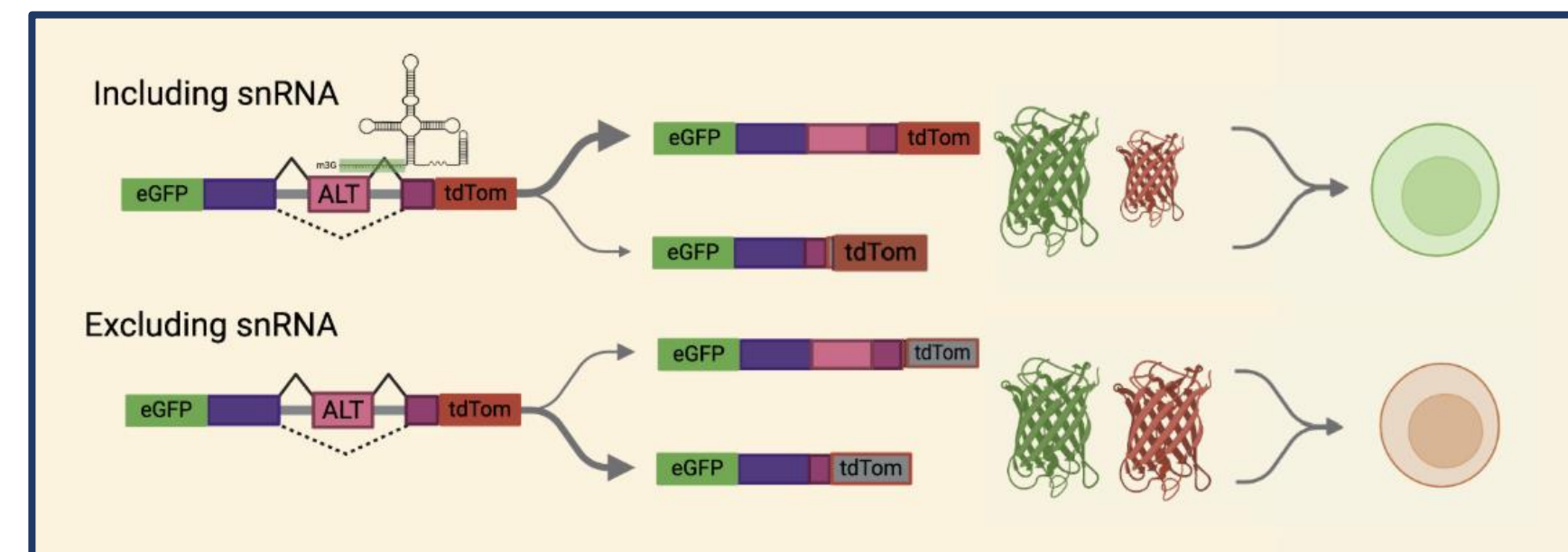


Figure 5. The dual ex MAPT reporter emits tdTomato (red) fluorescence when the exon is excluded and emits GFP (green) when the exon is included.

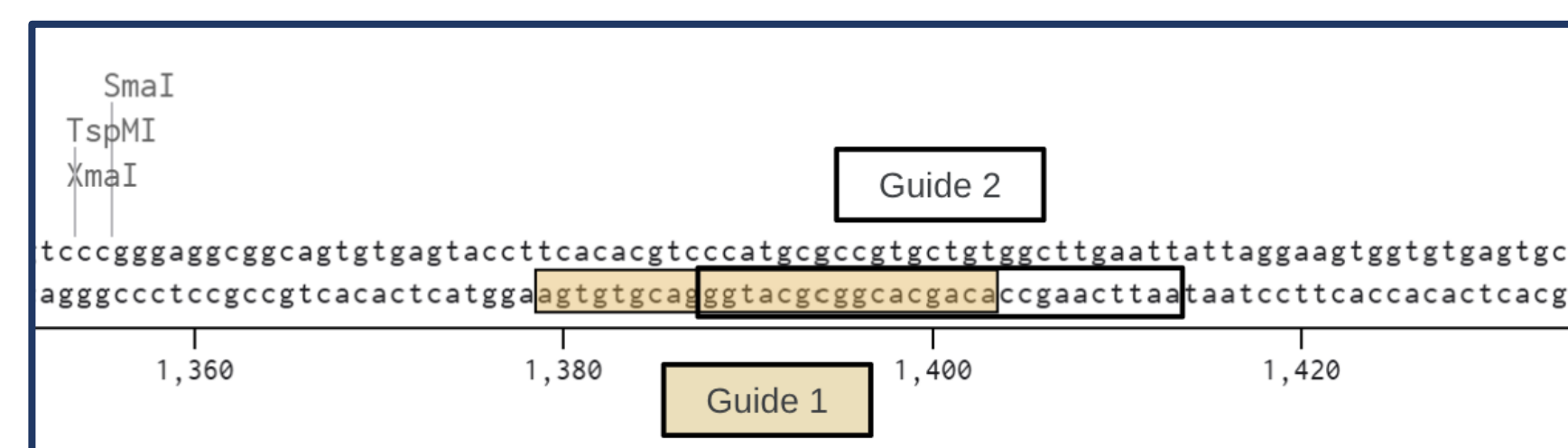


Figure 6. We tested two different guides, which bind to the exon at different points because their sequences represent different reading frames. This way we can also determine how different guides impact snRNA design.

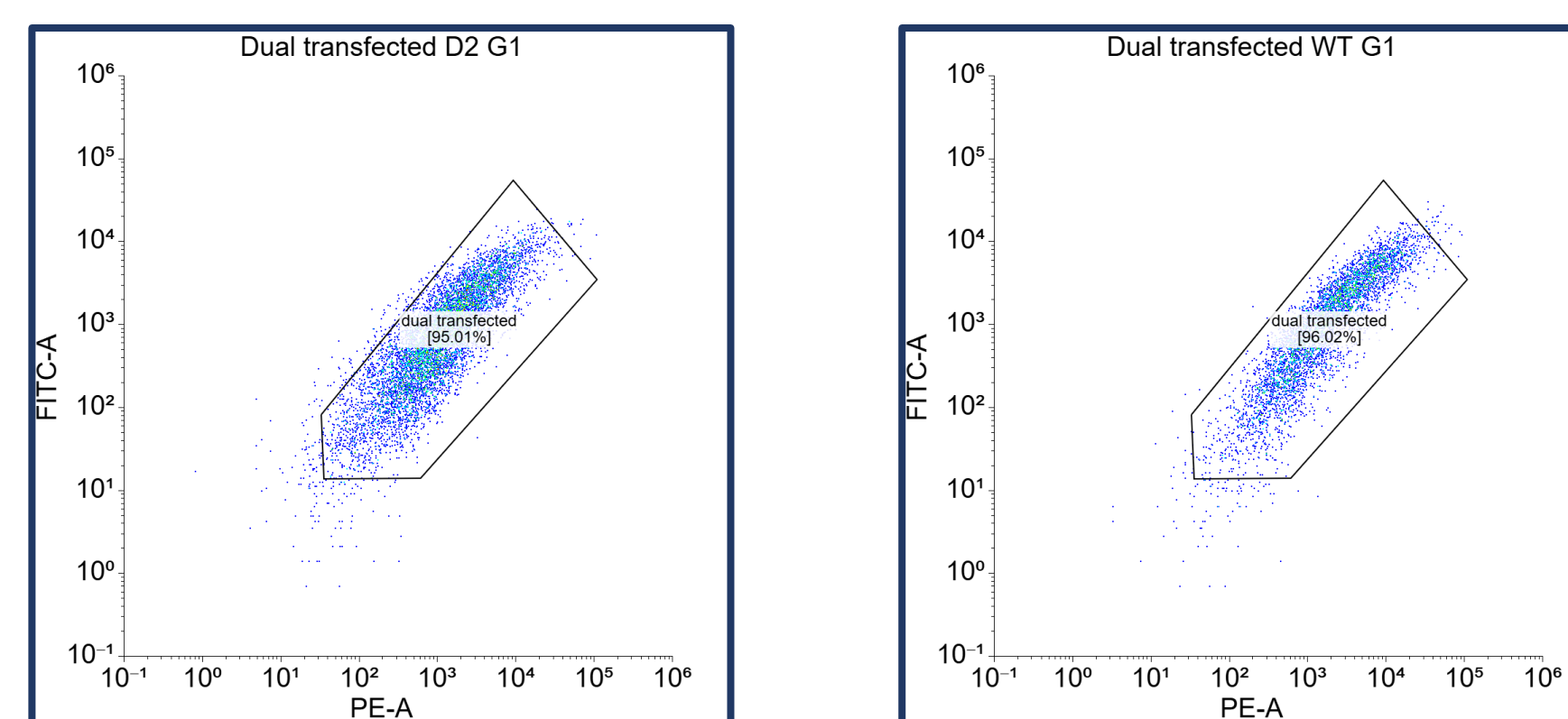


Figure 7. Flow cytometry scatter plots for wild type and a design. Design shows movement towards higher FITC and lower PE-A, as expected if the design is increasing exon inclusion.

Results

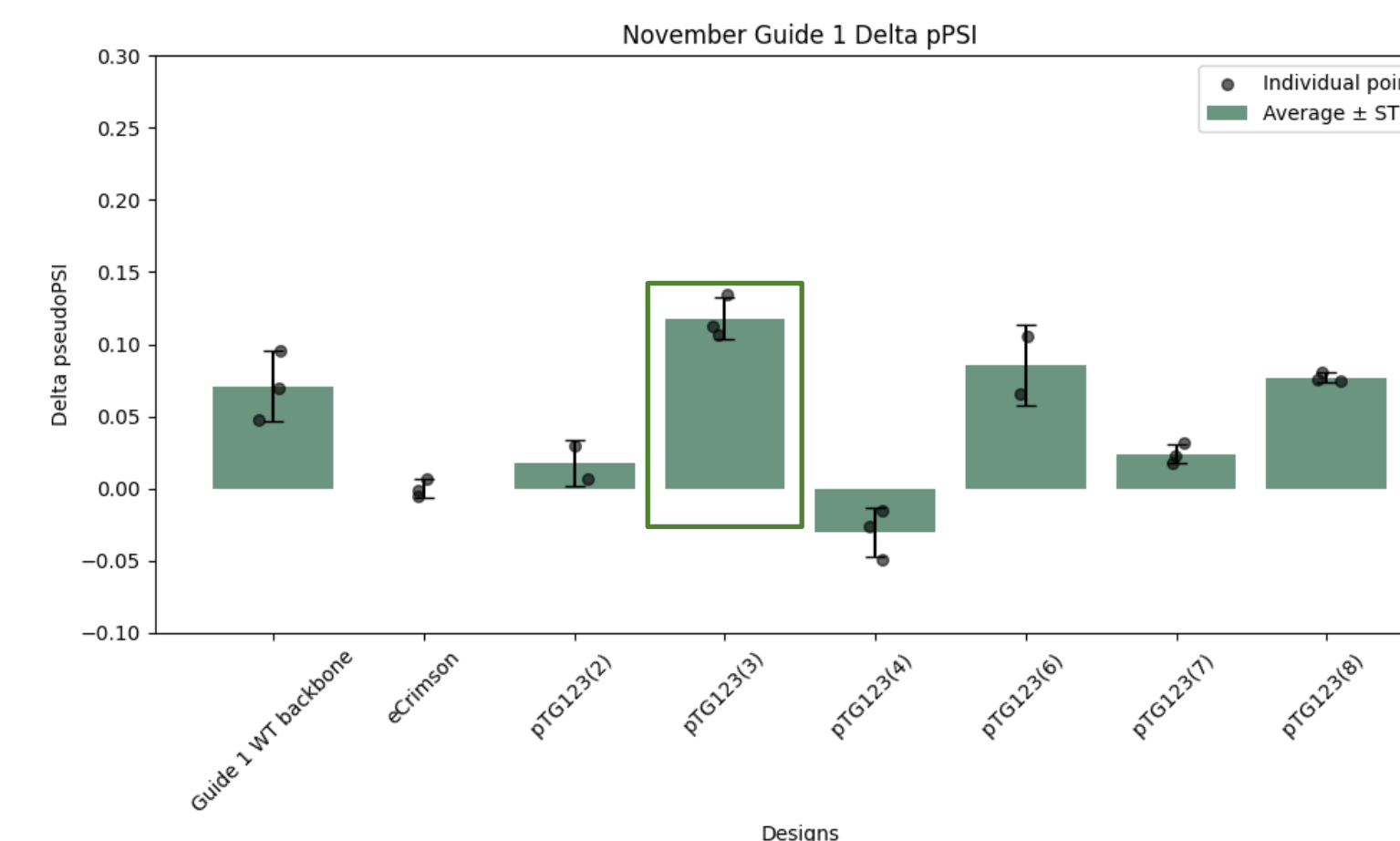


Figure 8. Design 3 has the most positive change in inclusion and outperforms the wild type by metric delta pseudo-PSI = $[1 - (PE-A/FIT-C)] / (NT \text{ AVG } PE-A/FIT-C)$ for guide 1.

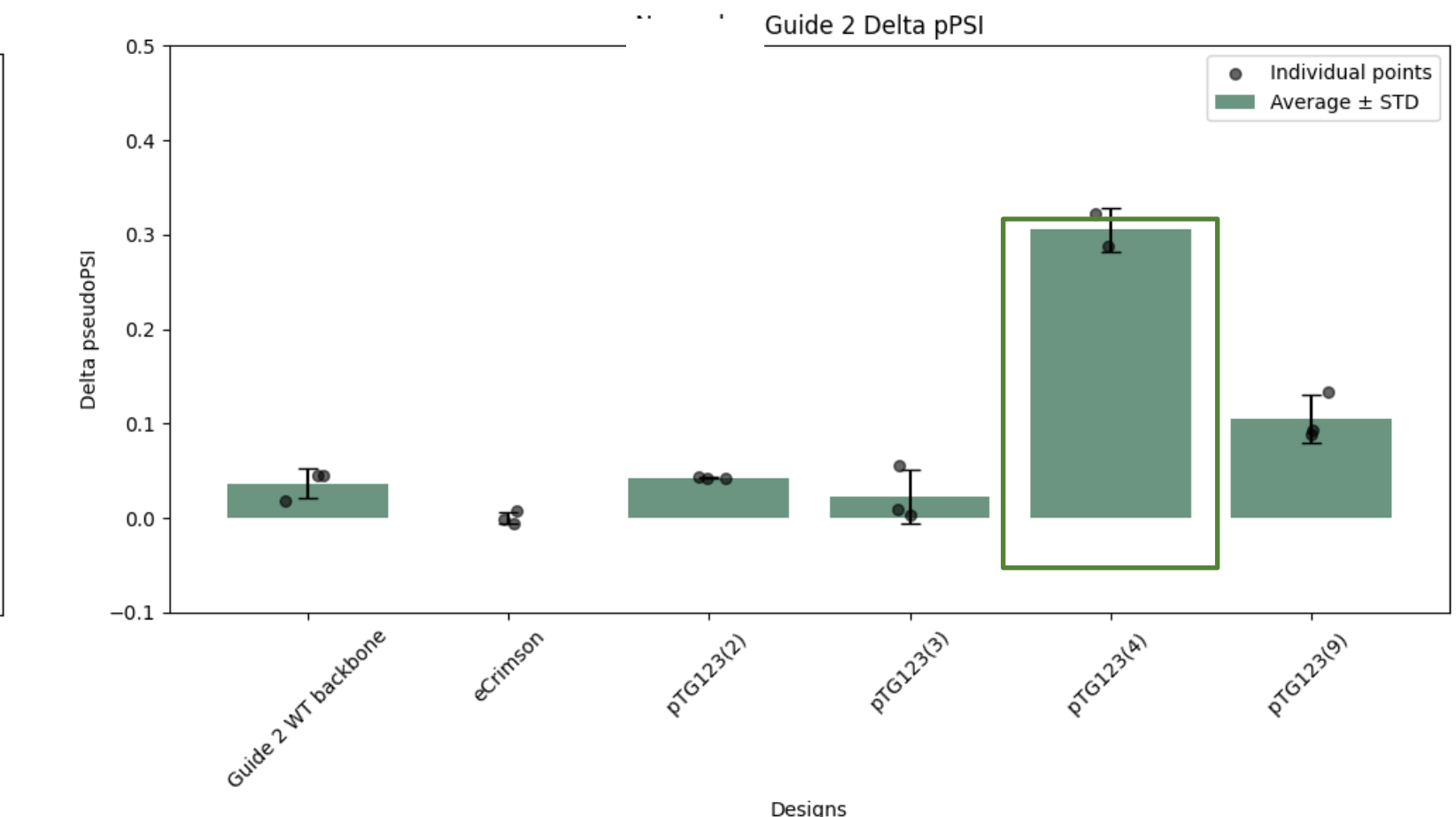


Figure 9. Design 4 has the most positive change in inclusion and outperforms the wild type by metric delta pseudo-PSI = $[1 - (PE-A/FIT-C)] / (NT \text{ AVG } PE-A/FIT-C)$ for guide 2.

Conclusions

Engineered U1 snRNA variants significantly modulated MAPT exon 10 inclusion in a guide-dependent manner. Two-tailed t-tests showed significant splicing changes relative to wildtype for Design 3/Guide 1 ($p = 0.0451$) and Design 4/Guide 2 ($p = 0.00121$). These results suggest that both snRNA structure and guide sequence influence exon inclusion efficiency. Future work will optimize lead designs, test disease-relevant models, and advance therapeutic RNA-based splicing correction strategies.

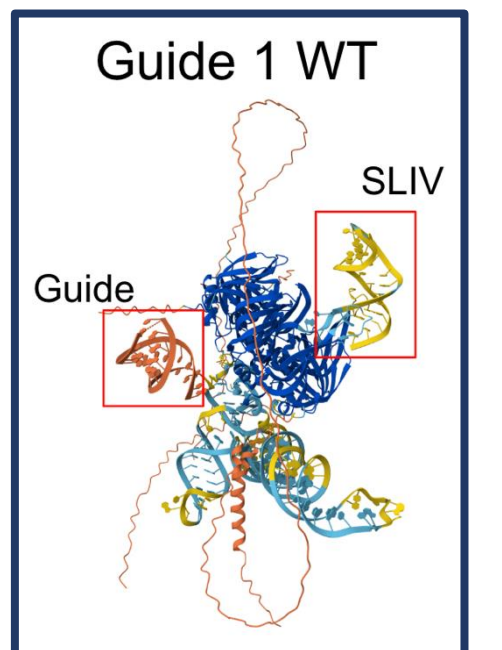


Figure 10. We used AlphaFold to predict snRNA structure with our inputted guides and designs.

Acknowledgements and References

We sincerely thank our mentor, Trent Gomberg, for his invaluable guidance and support throughout this project. We wanted to extend our thank you to Dr. Taylor and the TA team for their consistent encouragement, as well as Gene Yeo, our Principal Investigator.

